Critical behavior in annealed and unannealed crystals of benzil

A. Yoshihara, E. R. Bernstein, and J. C. Raich

Critical behavior in annealed and unannealed crystals of benzil[a]

A. Yoshihara, E. R. Bernstein, and J. C. Raich

Department of Chemistry and Physics, Colorado State University, Fort Collins, Colorado 80523

Simultaneous Brillouin-correlation light scattering results obtained under an external applied stress pulse are presented for annealed and unannealed (as grown) crystals of benzil. Critical fluctuations are characterized for the LA a-axis mode governed by the elastic constant c_{11} and are shown to contribute to this elastic anomaly in the high temperature phase. Both a central peak intensity anomaly and a critical relaxation time anomaly are characterized for unannealed crystals. These effects disappear in well-annealed crystals and without the external stress pulse even in as grown crystals. The critical relaxation behavior in benzil is coupled to the external stress compression wave generated by the mechanical refrigerator used to cool the sample. The latter interaction and relaxation anomaly are observed in polarized scattered light with the stress applied along the b (or a) axis as required for a c_{11} coupling. These observations are qualitively analyzed employing the theory of anelastic solids with higher order fluctuation terms incorporated into the free energy expansion. The relationship of this description to the Halperin–Varma theory of defect induced central peaks is outlined.

I. INTRODUCTION

Benzil $(C_6H_5CO)_2$ is a molecular crystal which has a crystallographic phase transition at ~83.5 K. Since the discovery of this phase transition through birefringence studies,[1] many experimental techniques have been employed to investigate this system.[2-8] The high temperature phase has been determined to possess a trigonal structure $D_3^4(P3_1 21)$ with three molecules/unit cell. The low temperature phase structure is assigned as $C2$.

The high symmetry phase of benzil is piezoelectric and the phase transition can be considered a ferroelectric–ferroelastic transition although the dielectric anomaly is quite weak. However, a symmetry argument based on molecular arrangement suggests that the spontaneous polarization due to the permanent dipole moment of the benzil molecule cannot be reversed by an external electric field. Benzil can thus be considered as belonging to the class of pyroelectric crystals.

Raman scattering[5] and infrared spectroscopy[6] have characterized a soft E mode which splits in the low symmetry phase. Moreover, Brillouin studies[7,8] reveal soft transverse acoustic (TA) phonons governed by an elastic instability in c_{44} and a soft longitudinal acoustic (LA) phonon governed by an elastic instability in c_{11}. A Landau mean field theory fully accounts for the TA soft phonon behavior but cannot account for the c_{11} anomaly.[8]

Actually, the c_{11} elastic constant can be decomposed into two independent contributions, $\frac{1}{2}(c_{11}+c_{12})$ and c_{66} as follows:

$$c_{11} = \tfrac{1}{2}(c_{11}+c_{12}) + \tfrac{1}{2}(c_{11}-c_{12}) = \tfrac{1}{2}(c_{11}+c_{12}) + c_{66} \quad .$$

c_{66} evidences some softening, but it is too weak to account for the entire c_{11} anomaly. The $\frac{1}{2}(c_{11}+c_{12})$ elastic constant is defined as the coefficient of $(e_1 + e_2)^2$ in the elastic energy expression for D_3 symmetry; the strain $(e_1 + e_2)$ is one of the elastic basis functions transforming

according to the irreducible representation A of the group D_3. Group theory predicts that any bilinear coupling between this basis and the E-symmetry order parameter is forbidden; the allowed coupling in lowest order is an electrostrictive-type interaction $A \otimes [E^2]$ in which the [ ] signifies the symmetric square. The explicit expression of this interaction is given by[8]:

$$(e_1 + e_2)(Q_1^2 + Q_2^2)$$

in which Q_1 and Q_2 represent components of the doubly degenerate E-symmetry order parameter. Through this coupling, $\frac{1}{2}(c_{11}+c_{12})$ possesses a critical anomaly which is stronger than the c_{66} anomaly and accounts for the c_{11} observed behavior. The above interaction also introduces a step discontinuity in the elastic constant at the transition temperature. The observed discontinuity substantiates a strong anharmonic fluctuation dominated interaction (See Fig. 2 of Ref. 8). Brillouin scattering experiments have consequently revealed a clear deviation from mean field Landau behavior in this molecular crystal.

An x-ray diffraction experiment[3] in the low temperature phase at ~74 K suggests a broken translational symmetry. Toledano[9] has developed a theory for the phase transition based on the observed broken translation symmetry in the (0001) plane of the hexagonal cell. Toledano introduced a three-dimensional Brillouin zone boundary order parameter (at the M point) which is assumed to be driven by the zone center instability through anharmonic interactions.

Reference 8 discusses the observed elastic anomalies and the zone center instability employing a Landau mean field theory developed for a ferroelastic phase transition in D_{3d} symmetry. It also treats qualitatively a contribution to the c_{11} anomaly due to the zone boundary order parameter; it is demonstrated in Ref. 8 that both zone boundary and zone center contributions to the c_{11} behavior have the same form for the anharmonic coupling interactions considered. Unfortunately, elastic measurements mentioned above cannot distinguish which contribution is more important.

In the past ten years, a number of studies have demonstrated that, in systems with a soft phonon response function, central peaks [large increases in Rayleigh intensity as $(T - T_c) \sim 0$] can be observed. The initial report of this phenomenon was for a neutron scattering study of $SrTiO_3$.[10] Since then, many experimental observations and theoretical models have appeared dealing with this manifestation of critical behavior.[11] Phenomenologically, the central peak can be understood as a consequence of bilinear coupling between soft mode(s) and a relaxator. Heat diffusion modes, microdomain motion, and defect motion have been considered as possible candidates for the relaxator.

Brillouin scattering is one of the most powerful techniques for the study of critical phenomena. The first report of a central peak observed by Brillouin scattering is due to Lagakos and Cummins[12] on the ferroelectric phase transition in KH_2PO_4(KDP). Since this discovery, the most extensive investigations on the origin of this phenomenon in KDP have been carried out by the Cummins et al.[13,14] Durvasula and Gammon,[15] Courtens,[16] and Courtens and Gammon.[17] Durvasula and Gammon argued that the central peak is VH polarized and static in origin as "speckle" interference fringes are observed around the transition point. These authors suggested that "static" defects are responsible for the central peak observations in KDP and suggested that natural abundance deuterium substituted for hydrogen in the crystal was the important defect. Courtens[16(a)] developed a mean field theory based on this point of view and was able to explain quantitatively the relative strength and temperature dependence of the observed central peak phenomena; these ideas and results, however, are not substantiated by further experiments.[16(b)] Courtens[16(b)] also confirmed that the KDP central peak can be strongly suppressed by annealing. For annealed crystals (140 °C, 18 h), only a uniform laser light column could be observed in VH or polarized light even at $T_c + 0.3$ K. This is to be contrasted with the static defect induced speckle interference pattern observed in as grown samples.

Mermelstein and Cummins[13] observed a new central peak in KDP just below the transition temperature. The new central peak is considered to be due to coupling between the ferroelectric soft mode and the thermal diffusion mode through the temperature dependence of the order parameter. Unlike the aforementioned static central peak, this phenomenon is considered to be a dynamic central peak. The dynamic central peak is forbidden in the high symmetry (high temperature) phase because the soft mode and thermal diffusion mode possess different symmetry. Applying an external electric field to KDP and thereby reducing the high temperature phase symmetry, Courtens[16(c)] found that the specific heat and thermal diffusivity extrapolated to zero field are temperature independent immediately above the transition.

Similar phenomena have been observed in $KH_3(SeO_3)_2$ (KTS) by Yagi et al.[18] The central peak in this crystal is VV polarized and strongly depends on the history of the sample. Even though KTS has a soft mode which can be observed in VH polarization, the polarization for the central peak suggests that there is no direct coupling between the "central mode" and the soft mode. On the other hand, similar soft TA mode and central peak behavior have been observed for the deuterated salt in VH polarization. This central peak is independent of the history of the sample. Moreover, highly deuterated samples evidence less divergent behavior. The origin of the DKTS central peak phenomena is considered to be the presence of impurities (protons) which can couple to the soft $x-y$ shear mode.[19] Although the origin for the KTS behavior is not yet apparent, inhomogeneous strains introduced in the process of crystal growth and shaping have been suggested as a possibility.

Lead germanate $Pb_5Ge_3O_{11}$ is another well-studied crystal which exhibits both static and dynamic central peak phenomena in light scattering spectra.[20] Lyons and Fleury assigned the dynamic central peak in this system, which shows a log (T_c-T) divergence, as related to the soft mode phonon density fluctuations interaction proposed by Cowley and Coombs.[21] They further assigned a static central peak which displays a power law temperature dependence with index 0.85 ± 0.2 as due to static symmetry breaking defects. The width of the dynamic central peak is as low as 4 GHz near T_c and the width of the narrow (static) central peak is less than 2 MHz and unresolved by Brillouin techniques.

In addition to studies by Fabry–Perot Brillouin scattering techniques, more direct approaches to the resolution of the narrow width of the central peak have been pursued for KDP,[22] quartz,[23] and $Pb_5Ge_3O_{11}$.[24] Unfortunately, no correlation function could be observed in a range of 1Hz–50 MHz. To the best of our knowledge, successful observation of the central mode (dynamic or static) by photon correlation spectroscopy has not as yet been reported. Using small angle scattering, it is possible to cover the time domain in which dynamical central modes are to be expected, at least around the transition temperature. At present, it is not understood why central peaks have not been observed by correlation spectroscopy under these conditions.

A theory of the defect induced central peak has been developed by Halperin and Varma.[25] They classify defects by the symmetry of the occupied site and the dynamics of the entire cell and calculate structure factors in two cases. For the "relaxing defect cell," theory predicts a narrow central peak with a width given by a renormalized relaxation time and a pair of soft phonon features. The defect cell stabilizes the low temperature structure due to a tendency of all the defects to order in such a manner as to favor the same orientation of the order parameter. The actual defect generated transition temperature is higher than the perfect crystal transition temperature. For the "frozen impurity" model, the defect or impurity merely fluctuates about its position and the obtained transition temperature becomes lower than the perfect crystal one. The dynamical structure factor in this case consists of three components: a zero width central peak for which the intensity diverges as $T \to T_c$; a finite width

central peak for which the width decreases as $T \rightarrow T_c$; and a pair of phonon peaks for which the frequency decreases as $T \rightarrow T_c$ initially, but then begins to increase before T_c is reached. The experimental results already discussed seem to be consistent with a general relaxing defect model.

Recently, a neutron inelastic scattering experiment revealed a central peak response in addition to a soft mode rotational response near a structural phase transition in another molecular system, chloranil.[26]

During the course of our Brillouin investigations on benzil, the Rayleigh intensity, as observed in the Brillouin spectra along the a axis, was found to show a rapid enhancement just above the transition temperature $[(T - T_c)/T_c \lesssim 2 \times 10^{-2}]$. A similar, but less pronounced, central peak associated with a soft TA-mode response was observed in the ferroelastic phase transition in sym-triazine by Brillouin scattering.[27] An attempt was also made to detect a relaxation mode by correlation spectroscopy covering the time domain between 1 and 10^{-6} s. Unfortunately, no relaxation process could be detected within this range for the triazine transition.

In this report, we will present more extended investigations of the central peak in benzil by Brillouin scattering and correlation spectroscopy achieved under an external applied stress pulse. It is found that observation of the central peak response in benzil is strongly coupled to not only crystal quality, but also the external pulse. In the presence of the external stress pulse, "as grown" samples show a central Rayleigh intensity peak at T_c, while well annealed crystals do not. Correlation spectroscopy reveals that, in as grown but not in annealed crystals, a critical (slow) relaxation is excited if a periodic external direction dependent stress is applied to the crystal. This relaxation or correlation time can be modeled by an anisotropic structural defect in the crystal employing the theory of anelastic solids. It is concluded that in order for the critical dynamics of benzil to be manifested in the Rayleigh central response light scattering spectrum, amplification through a local stress/dielectric tensor inhomogeneity is apparently necessary. Similar results have also been observed for chloranil and will soon be reported in a separate publication. Negative results of such experiments are also discussed for NH_4Cl and triazine. Urea, which does not undergo a phase transition between 300 and 15 K, evidences an external stress related correlation function but without any anomalous temperature behavior.

II. EXPERIMENTAL

The experimental apparatus for the Brillouin scattering and correlation spectroscopy is such that both measurements can be made simultaneously by splitting the scattered light. Figure 1 shows an optical diagram of this apparatus, including the data acquisition systems. Details of the Brillouin scattering system alone have been already reported.[8] For the simultaneous measurement of Brillouin and correlation spectra, a beam splitter is placed behind a pinhole and the resultant beams are introduced into each arm of the Brillouin/
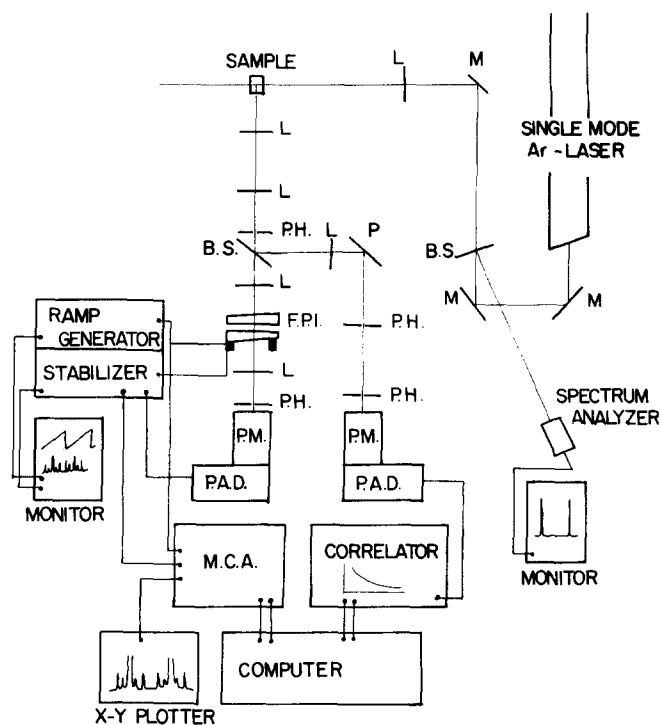

FIG. 1. Optical diagram and data acquisition system for the simultaneous measurement of Brillouin scattering and correlation spectroscopy. Notation: L = lens, P.H. = pinhole, M = mirror, P = prism, B.S. = beam splitter, P.M. = photomultiplier tube, and P.A.D. = preamplified/discriminator.

correlation spectrometer. It has been found that such a measurement procedure is necessary to obtain reproducible results and to obtain proper correlation intensity.

Apparatus for correlation spectroscopy is quite simple and consists of a pair of pinholes (500 μm diameter each) spaced 20 cm apart and followed by a thermoelectrically cooled photomultiplier tube (RCA C31034A-02). A lens is placed just behind the beam splitter to increase signal and a narrow band filter for 5145 Å is placed in front of the pinholes to attenuate Raman scattered and fluorescence light from the sample. Pulses from the phototube are amplified and discriminated and then fed into a real time autocorrelator (Malvern K7025). The 64 channel correlator has a range of sampling times from 10^{-7} to 10^{-1} s, effectively covering a time domain between 10^{-6} and 1 s. The correlator has two modes of operation for autocorrelation: a zero clipped correlation mode and a full correlation mode. In this benzil study, the full correlation function mode was employed.

A desk top computer (HP 9845S) controls both the correlator for Rayleigh scattering and the multichannel analyzer for Brillouin scattering experiments. The computer accepts a data set from the correlator at the end of a preset experimental detection time and calculates the intensity autocorrelation function by a least squares fitting technique employing the simple form

$$g^{(2)}(t) = 1 + \delta + Ae^{-2t/\tau} ,$$

in which A, δ, and τ are the fitting parameters.[28] A finite value of δ can be due to real scattering processes
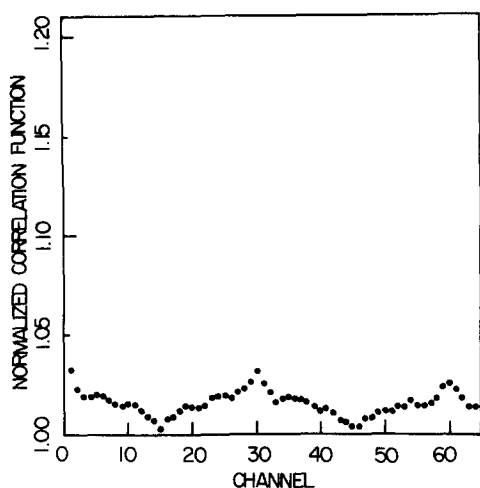
FIG. 2. Intensity correlation function for benzil at very low frequency showing the 3.3 Hz modulation applied to the sample through the refrigerator. Sampling time is 10^{-2} s and the correlation function is repeated each 30 channels. Thus, one period corresponds to $10^{-2} \times 30 = 0.3$ s. The parasitic shock wave which causes the stress pulse to the sample occurs on a much faster time scale as described in the text.

with larger relaxation times relative to the one being studied, to misnormalizations caused by fluctuations in laser intensity, or to other external sources. We will discuss this point more fully below.

The coefficient A has a value between 0 and 1 depending on sampling time T_s, dead time T_d, and pinhole size. For the full correlation function mode of operation, the A factor can be expressed by a product of three independent contributions as follows[29]:

$$A = A_1(\tau_c/T_s) A_2(T_s/T_d) A_3(S_{coh}/S) ,$$

in which τ_c is the coherence (relaxation) time, S_{coh} is the coherence scattering area $(S_{coh} = \lambda^2/d\Omega)$, and S is the effective detector area. For larger values of τ_c/T_s and T_s/T_d, A_1 and A_2 approach unity. On the other hand, A_3 approaches unity for $S_{coh}/S > 1$ and approaches S_{coh}/S for $S_{coh}/S \ll 1$.

The actual experimental conditions are

$$\tau_c/T_s \sim 60 , \quad T_s/T_d \sim 10 , \quad \text{and } S_{coh}/S \sim 1/7 .$$

In an experiment, the A factor will be determined mainly by $A_3(S_{coh}/S)$ and is approximated by

$$A \approx \frac{S_{coh}}{S} \sim 0.15 .$$

Changing the 500 μm pinholes to 200 μm pinholes causes the A valve to increase, but the signal level to decrease; the 500 μm pinhole set was used throughout the experiment. Estimated error (standard deviation) in the calculated relaxation time is about ±10%.

Single crystals of benzil are grown from xylene saturated solutions by slow evaporation. Two different types of 90° scattering samples were prepared: "as grown" from solution and annealed at 50 °C for ~48 h.

A closed cycle He refrigerator (CTI 21) is used to

obtain temperatures as low as 15 K. The sample is affixed to a copper block using G.E. varnish 7031 and then placed in a copper scattering cell wrapped with a heater. Temperature is controlled with a proportional controller through a sensor diode placed on the copper cell. A copper–constantan thermocouple is placed just below the sample and affixed to it by varnish in order to measure temperature at the sample more precisely. Temperature fluctuation during the data accumulation time of about one hour is no more than ±1 μV or about 0.05 K around 80 K.

Each refrigerator cycle is roughly 0.3 s long (3.3 Hz engine). A correlation function due to this engine cycle is represented in Fig. 2. For shorter sampling time measurements, this refrigerator correlation function is superimposed on the sample related correlation function and gives a finite value to the parameter δ as already discussed. In addition to this engine cycle, the refrigerator inputs two transient pulses to the sample. As compressed He gas expands during the closed cycle cooling process, the gas absorbs heat from the sample and the sample is cooled. The sample thereby receives a negative heat pulse during this expansion portion of the cycle. It is estimated that this pulse corresponds to a ΔT of less than 0.02 K under constant temperature conditions around the transition temperature. Simultaneously with this temperature pulse, a fast parasitic shock wave is created by the expansion process and propagates through the system. The sample is compressed by this shock wave at the end of each cycle. The parasitic shock wave can be thought of as a square wave of duration $\sim 10^{-2}$ s with a time rate of change in the 10–100 μs range. This shock wave compression is the most important external factor in our experiment and will be discussed further in Sec. IV.

III. RESULTS

Figure 3 shows an example of the correlation function in a benzil as grown crystal at 83.4 K (about 0.1 K below T_c). The full line is a least squares fit result of the form
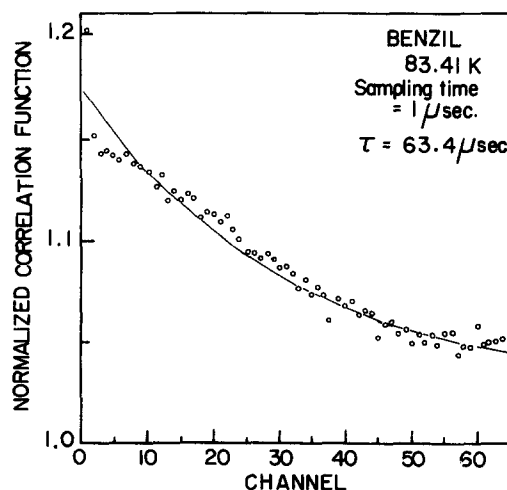

FIG. 3. Benzil relaxation function obtained just below the transition temperature $(T_c - T \sim 0.1 \text{ K})$. Sample is unannealed and the stress σ_2 is applied along the b-axis.
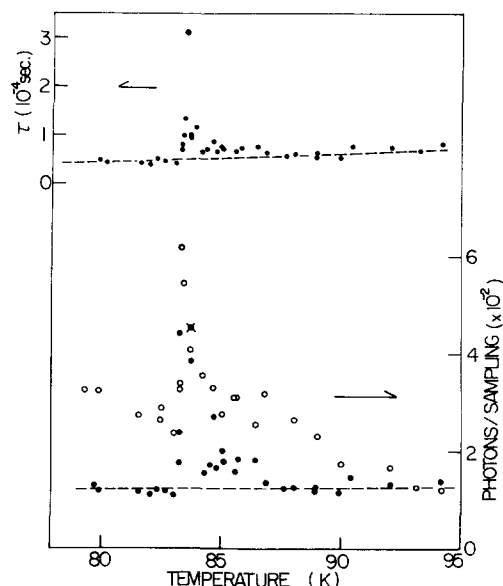
FIG. 4. Temperature dependence of the relaxation time and counting rate/sampling time for an as grown crystal. Broken lines show base lines for the relaxation time (τ_e) and counting rate assuming that they would not change at T_c. Full circles for the counting rate results were calculated from the anomalous part of the relaxation time using Eqs. (14) and (22). The calculated value at 84 K shown by ⊗ was used to normalize the result. The relaxation time and the intensity anomaly are thus strongly correlated with one another as indicated in the text [see Eqs. (22) and (23)]. Structure in both plots is reproducible over various samples and for a single sample at many positions across a crystal face.

$$g^{(2)}(t) = 1.03 + 0.15 \exp(-2t/63 \ \mu s)$$

with standard deviation 0.7×10^{-3}. The correlation function could be observed in *polarized scattered light* only. Temperature dependence of the relaxation time and pulse counting rate/sampling time are given in Fig. 4 for this scattering configuration. The relaxation time shows a weak and monatomic temperature dependence above 88 K. Below the transition temperature (~ 83.5 K), this relaxation time becomes temperature independent and has a value of about 40 μs. The relaxation time anomaly has an asymmetric tail on the high temperature side between the transition temperature and 88 K. In addition, the pulse counting rate, which is equivalent to the Rayleigh intensity in Brillouin spectra, shows a stronger temperature dependence over a wider temperature range. This intensity has a sharp asymmetric peak centered around the transition temperature.

In the low temperature phase the Rayleigh intensity gradually increases again due to domain scattering. This intensity result is consistent with our previous Brillouin scattering measurement which also reveals the central peak. (See Fig. 3 of Ref. 8 and Fig. 6 of this paper). These features, as observed in correlation spectroscopic studies, have good reproducibility except in the critical region ($T_c \pm 1$ K). Within this "critical region," the above mentioned anomalies are strongly sample dependent and results for the relaxation time are shown in Fig. 5.

In an attempt to ascertain the source of this correla-

tion function, the refrigerator compressor was turned off and the correlation function was remeasured. *It is found that no correlation function is observed during the time the refrigerator compressor is off.* However, upon restarting the refrigerator, the correlation function is recovered. During the time the refrigerator is off, the sample temperature increases considerably (~ 50 K). In the high temperature phase, the relaxation time measured is almost constant at roughly 65 μs. Thus, the temperature during the refrigerator off period should not significantly affect the value of τ_c and certainly should not make it zero. Moreover, if the experiment is carried out ~ 300 K, at which temperature little drift in temperature can take place, similar results are obtained. Therefore, the observed correlation function is not an intrinsic property of benzil, but rather a compressor induced extrinsic effect.

The refrigerator imparts to the sample two types of pulses, heat and stress, as has already been pointed out. The order of magnitude of the temperature disturbance due to the negative heat pulse has been estimated to be about 0.02 K and it is of the order of the temperature fluctuation at the sample position. Even the much larger temperature disturbance induced by turning off the compressor did not induce any observable correlation function. Thus, the stress pulse seems to be the important one.

The Brillouin and Rayleigh experiments have been repeated using annealed crystals in the same scattering geometry. *The correlation function and central peak could not be observed for well annealed samples with the refrigerator either on or off.* Brillouin scattering results are presented in Fig. 6 with our previous results.[8] As the propagation direction in this experiment was slightly tilted from the [100] to [001] direction, the TA "[100]" phonon frequency (X) shows a higher, but parallel, shift with respect to the previous results ($\sim 5\%$). The other measurement (+), associated with a better
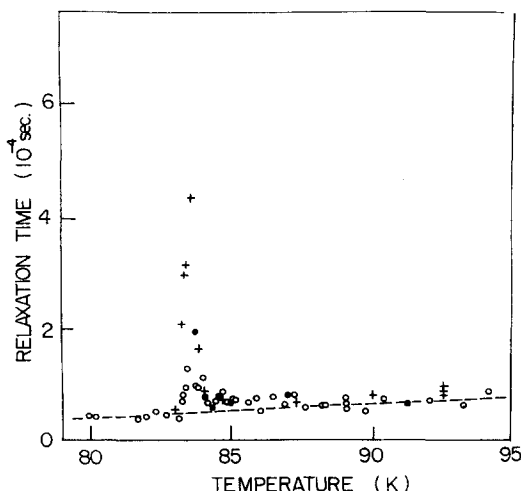

FIG. 5. Temperature dependence of the relaxation time as observed in three grown samples. Results of one of these samples (●) are the same as presented in Fig. 4. One can readily see that there is a strong sample dependent critical behavior in unannealed crystals. The broken line is the same base line drawn in Fig. 4.
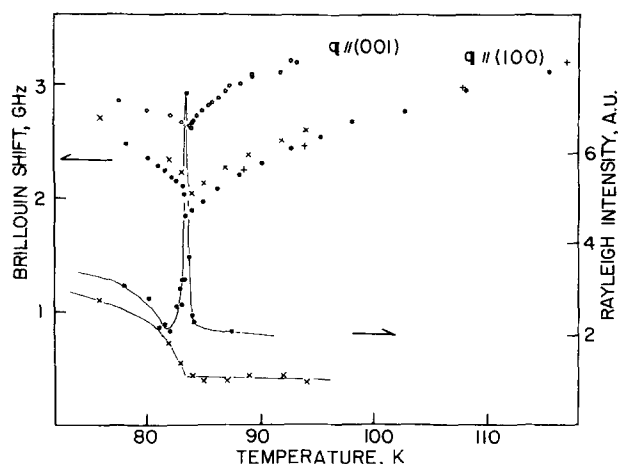
FIG. 6. Brillouin scattering results for well-annealed and unannealed samples. Frequency shifts of the lowest energy photon and Rayleigh intensity measurements are shown with our previous results on as grown samples, as a function of temperature. Annealed samples are indicated as (×) and (+). The results for the × sample were obtained on a phonon for which the propagation direction was slightly tilted from the [100] direction towards the [001] direction. The frequency of this TA mode is uniformly increased about 5%. No correlation function could be observed in these annealed samples and they did not show a central Rayleigh intensity peak.

oriented sample, is in good agreement with those of Ref. 8. The well annealed samples evidence no central peak. Annealing effects and sample dependent critical behavior suggest that defects or impurities in the as grown samples might be of the origin of the central peak in benzil.

In order to investigate stress direction dependence of the correlation function, samples which have *ac*-scattering plane and *ab*-scattering plane orientation were prepared from as grown crystals and examined by correlation spectroscopy from room temperature to 70 K. *It is found that well defined correlation function and intensity anomalies could be observed only in the ac-scattering plane geometry.* These geometries and results are summarized in Fig. 7.

The clear conclusion from the results of these measurements is that the refrigerator compression wave excites some motion of an annealable impurity/defect in the benzil crystal. The relaxation behavior of this defect generates a critical coupling between the order parameter and the elastic modes. This coupling is in particular important for the c_{11} related modes, which evidence fluctuation dominated behavior in addition to these annealable central peak effects.

In order to demonstrate that the observed correlation function and its temperature dependence are of a microscopic defect nature rather than a macroscopic (dust inclusions, cracks, etc.) nature, a number of additional experiments were performed. First, of course, are the anisotropy results and refrigerator on/off studies reported above. Second, the correlation function and intensity anomaly completely vanishes in annealed crystals, even though the microscopic appearance of

these samples in laser light is unchanged. Third, many large crystals were employed and the observations are in all instances constant over the entire crystal face studied and over many samples. Fourth, ammonium chloride and *sym*-triazine show no correlation function at all under any conditions. These materials have low Rayleigh to Brillouin intensity ratios of about 1–10. On the other hand, chloranil and urea evidence a correlation function associated with the refrigerator compressor operation. Chloranil, in addition, has a critical anomaly in the relaxation time and intensity that is nearly identical to that found for benzil considering crystal symmetry differences [$\tau(100$ K$) \sim 4$ ms and $\tau(90$ K$= T_c) \sim 7$ ms]. Since urea has no phase transition between 300 and 15 K that could be observed in Brillouin and correlation scattering, the relaxation time observed for urea did not show any anomalous temperature dependence [e.g., $\tau(15$ K$) \sim 1$ ms, $\tau(300$ K$) \sim 3$ ms]. Benzil, chloranil, and urea have unannealed Rayleigh/Brillouin intensity ratios about five to ten times larger than NH_4Cl and triazine, perhaps indicating the concentration of (annealable) defects is higher in these as grown samples. Fifth, it is to be emphasized that all these crystals are quite weak scatters as are most molecular crystals.

IV. DISCUSSION

In this description of the underlying causes for the observed benzil critical behavior, it is assumed that the zone center soft E optic mode observed by Raman scattering[5] and infrared spectroscopy[6] is the primary origin of the phase transition. In addition, the soft phonon amplitudes are chosen as the order parameters. The free energy for the high temperature phase can then be written,[8,30]

BENZIL	SAMPLE I	SAMPLE II
SCATTERING PLANE	ac	ab
PHONON DIRECTION	[100]	[100]
EXCITED STRAIN	e_2	e_3
SYMMETRY	A + E	A
CORRELATION FUNC.	OBSERVED	NOT OBSERVED
POLARIZATION	Hh	

$$e_2 = \underbrace{\left(\frac{e_1 + e_2}{2}\right)}_{A} - \underbrace{\left(\frac{e_1 - e_2}{2}\right)}_{E}$$

FIG. 7. Relation between direction of applied stress (from the refrigerator) observation of the correlation function and the crystal axes. The stress direction is represented by the arrow pointing down and the scattered light observation direction is given by the arrow coming out of the page. The incident light is indicated by the arrow perpendicular to these two.

$$F = F_0 + \tfrac{1}{2} a(Q_1^2 + Q_2^2) + \tfrac{1}{3} b(Q_1^3 - 3Q_1 Q_2^2) + \tfrac{1}{4} c(Q_1^2 + Q_2^2)^2 + \frac{1}{2} \left(\frac{c_{11}^0 + c_{12}^0}{2}\right)(e_1 + e_2)^2 + \tfrac{1}{2} c_{33}^0 e_3^2 + \tfrac{1}{2} c_{44}^0 (e_4^2 + e_5^2) + \tfrac{1}{2} c_{66}^0 (e_6^2 + e_7^2)$$

$$+ c_{13}^0 (e_1 + e_2)e_3 + c_{14}^0 (e_4 e_7 - e_5 e_6) + A(e_4 Q_1 - e_5 Q_2) + B(e_7 Q_1 + e_6 Q_2) + C(e_1 + e_2)(Q_1^2 + Q_2^2) + \cdots \tag{1}$$

in which $a = a_0(T - T_0)$, $e_7 = e_1 - e_2$, and $c_{66}^0 = (c_{11}^0 - c_{12}^0)/2$. This free energy expression predicts triple twinning (domain formation) in the low temperature phase and one can put $Q_2 = e_5 = e_6 = 0$ for the domain I without loss of generality. The simplified free energy takes the form

$$F = F_0 + \frac{a}{2} Q_1^2 + \frac{b}{3} Q_1^3 + \frac{c}{4} Q_1^4 + \frac{1}{2}\left(\frac{c_{11}^0 + c_{12}^0}{2}\right)(e_1 + e_2)^2 + \tfrac{1}{2} c_{44}^0 e_4^2$$

$$+ \tfrac{1}{2} c_{66}^0 e_7^2 + c_{14}^0 e_4 e_7 + A e_4 Q_1 + B e_7 Q_1 + C(e_1 + e_2)Q_1^2 + \cdots . \tag{2}$$

For a free crystal $\partial F/\partial Q_1 = 0$, two independent elastic instabilities result from the bilinear coupling terms between the order parameters and strains e_4 and e_7. In the high temperature phase, these elastic instabilities are represented as

$$c_{44} = \frac{\partial^2 F}{\partial e_4^2} = c_{44}^0 - \frac{A^2}{a} = c_{44}^0 \frac{T - T_1}{T - T_0} \tag{3}$$

and

$$c_{66} = \frac{\partial^2 F}{\partial e_7^2} = c_{66}^0 - \frac{B^2}{a} = c_{66}^0 \frac{T - T_2}{T - T_0} \tag{4}$$

with

$$T_1 = T_0 + \frac{A^2}{a_0 c_{44}^0}$$

and

$$T_2 = T_0 + \frac{B^2}{a_0 c_{66}^0} .$$

On the other hand, the elastic constant $(c_{11} + c_{12})/2$ does not evidence an anomaly within the Landau theory; i.e.,

$$\frac{c_{11} + c_{12}}{2} = \frac{\partial^2 F}{\partial(e_1 + e_2)^2} = \frac{c_{11}^0 + c_{12}^0}{2} . \tag{5}$$

In our previous Brillouin scattering experiments, the temperature dependence of c_{11} was measured. As pointed out in the Introduction, behavior of c_{11} can be decomposed into contributions from two independent sources as follows:

$$c_{11} = \frac{c_{11} + c_{12}}{2} + \frac{c_{11} - c_{12}}{2} = \frac{c_{11} + c_{12}}{2} + c_{66} . \tag{7}$$

Substituting the calculated effective elastic constants c_{66} and $(c_{11} + c_{12})/2$ into Eq. (7), one finds

$$c_{11} = \frac{c_{11}^0 + c_{12}^0}{2} - \Lambda_+ \left(\frac{T - T_0}{T_0}\right)^{-\rho_+} + c_{66}^0 - \frac{B^2}{a}$$

$$= c_{11}^0 - \frac{B^2}{a} - \Lambda_+ \left(\frac{T - T_0}{T_0}\right)^{-\rho_+} = c_{11}^0 \frac{T - T_3}{T - T_0} - \Lambda_+ \left(\frac{T - T_0}{T_0}\right)^{-\rho_+} \tag{8}$$

in which $T_3 = T_0 + (B^2/a_0 c_{11}^0)$. This is the same expression used to analyze the c_{11} anomaly in our previous report.[8] In Fig. 8, temperature dependence of c_{66} and $(c_{11} + c_{12})/2$ are shown. It is clear from the figure that $(c_{11} + c_{12})/2$ has the stronger anomaly. This elastic constant $(c_{11}$

$+ c_{12})/2$, is derived by calculation from the measured c_{11} and c_{66} values in a manner similar to that shown in Eq. (7).

The half-width of the LA phonon parallel to the [100] direction has an anomalous increase near the transition temperature.[8] This anomaly is also due to anharmonic interaction with the order parameter fluctuations. Since the imaginary part of c_{66} is always smaller than the real part (i.e., the TA phonon is always well defined and under damped), the half-width anomaly must be primarily associated with the imaginary part of the elastic constant $(c_{11} + c_{12})/2$. This can be written[31]

$$\mathrm{Im}\left[\frac{c_{11} + c_{12}}{2}\right] = \frac{\omega}{2k_B T}\sum_{qq'}' C(q) C(q')$$

$$\times \int_{-\infty}^{\infty} dt\, e^{i\omega t} \langle |Q_1(q, t)|^2 |Q_1(q')|^2 \rangle , \tag{9}$$

in which wave vector and time dependence have been introduced into the coupling coefficient C and order parameter Q_1 fluctuations. One can therefore conclude that the order parameter fluctuations play an important role in the dynamics of the phase transition in benzil.

Let us now turn to a discussion of the defect associated central peak and relaxation time anomaly in benzil. In the experiment using the closed cycle cryostat, external periodic stress is always applied to the sample. It should be emphasized here that: the correlation function could not be observed without the external pulse
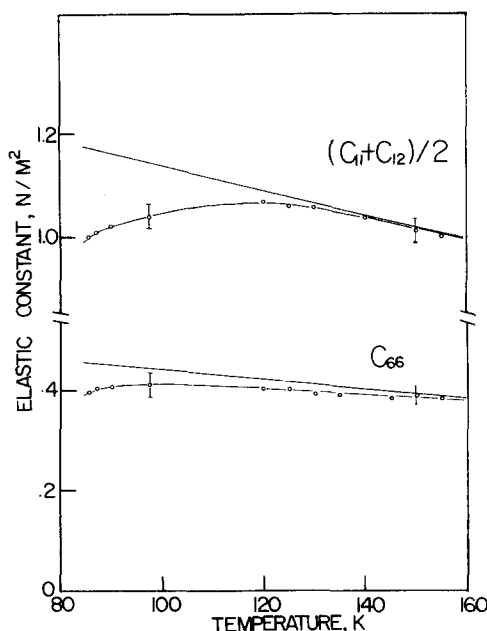

FIG. 8. Temperature dependence of the elastic constants $(c_{11} + c_{12})/2$ and c_{66}. The full straight lines are extrapolated from the high temperature limiting slopes. The vertical axis is in units of 10^{10} N/m^2.

from the refrigerator even around the transition temperature; the correlation function only appeared for unannealed samples; and the well-defined correlation function was observed only in specific directions associated with the c_{11} elastic constant already shown to evidence strong critical behavior. The first observation is consistent with the previous experimental results for correlation scattering in KDP, [22] quartz, [23] and $Pb_5Ge_3O_{11}$. [24] Although the correlation function is clearly induced by the external pulse, it is still possible that an intrinsic central peak for which a correlation function cannot be resolved by light scattering techniques does indeed exist in this system. Nonetheless, it is of considerable interest to understand how the external pulse induces the correlation function and by what mechanism the Rayleigh anomaly takes place around the transition temperature. Below a possible theoretical model description which can qualitatively explain the observed facts is presented. In this discussion, we employed the theory of anelasticity as the observations are for a system under periodic external applied stress. The relation between these ideas and those of the usual central peak defect theory will be presented after this development.

Under the above conditions, a low frequency dispersion will be induced in the elastic constants by the forced motion of the local field around an imperfection. Therefore, the theory of elasticity in a perfect crystal cannot model the actual experimental conditions. Instead, the theory of anelasticity [32] should be employed to account for the induced dispersion. A stress applied perpendicular to the ac plane σ_2 induces a combination of strains for benzil of the form

$$\sigma_2 = c_{12}e_1 + c_{11}e_2 + c_{13}e_3 - c_{14}e_4 . \tag{10}$$

As c_{12}, c_{13}, and c_{14} do not show any anomalies near the transition temperature, only the second term in Eq. (10) will be considered in the ensuing discussion. Thus, we set $\sigma_2 \approx c_{11}e_2$.

Following the theory of anelasticity, the above equation should be replaced by

$$\sigma_2 + \tau_e \dot{\sigma}_2 = c_{11}^R e_2 + \tau_e c_{11}^U \dot{e}_2 , \tag{11}$$

in which τ_e is the bare stress (constant strain) relaxation time, c_{11}^R is the relaxed (equilibrium) elastic constant defined by Eq. (8), and c_{11}^U is the unrelaxed elastic constant. For an unannealed sample, the complex elastic constant $c_{11}^*(\omega)$ can be defined to replace c_{11}^R and can be readily calculated by Fourier transformation giving

$$c_{11}^*(\omega) = c_{11}^R + \Delta c_{11} \frac{i\omega\tau_e}{1 + i\omega\tau_e} \tag{12}$$

in which $\Delta c_{11} = c_{11}^U - c_{11}^R$. We identify c_{11}^R with the observed elastic constant c_{11} for an annealed sample, as defined by Eq. (8).

In a discussion of the elastic constants obtained by these Brillouin scattering studies, one should use a dynamical theory with the above complex elastic constant instead of the static thermodynamic theory with the elastic constant c_{11}^R. However, the soft phonon fre-

quency is always much higher than the acoustic phonon frequencies obtained by Brillouin scattering and the soft mode can thereby follow the acoustic phonon motion. The low frequency dispersion in the order parameter/elastic mode coupling, therefore, has little effect on the soft acoustic phonon's response except in the Rayleigh response range ($\omega < 10^7$ Hz). Thus, to obtain the temperature-frequency dependent elastic constant $c_{11}^*(\omega, T)$, it is sufficient to replace c_{11}^0 in Eq. (8) by the complex elastic constant $c_{11}^*(\omega)$. This yields

$$c_{11}^*(\omega, T) = c_{11}^0 \frac{T - T_3}{T - T_0} - \Lambda_+ \left(\frac{T - T_0'}{T_0'}\right)^{-p_+} + \frac{i\omega\tau_e}{1 + i\omega\tau_e} \Delta c_{11}$$

in which T_0' is used instead of T_0 [as given in Eq. (8)] in the second term of Eq. (13). This latter substitution is intended to indicate all possible contributions of this general form, due to higher order fluctuation terms in the free energy, which should be included in the complex elastic constant $c_{11}^*(\omega, T)$.

According to Brillouin scattering selection rules for phonons propagating along the a axis, [33] only the LA phonon whose frequency is governed by c_{11} can be observed in the polarized scattering geometry for which both the correlation function and central peak have been uniquely observed.

The dynamic susceptibility of the LA phonon may be derived using Lagrange's equation of motion to obtain constitutive equations for the system. The result of such a calculation can be written as

$$\chi(q, \omega) = \frac{(q^2/\rho)}{(q^2/\rho)c_{11}^*(\omega, T) + i\gamma\omega - \omega^2}$$

$$= \frac{(q^2/\rho)}{\omega_a^2 + \Delta\omega_a^2 - \Delta\omega_a^2/(1 + i\omega\tau_e) + i\gamma\omega - \omega^2} , \tag{14}$$

in which the acoustic phonon frequency ω_a and the shift $\Delta\omega_a$ are given by

$$\omega_a^2 = (q^2/\rho)\left[c_{11}^0 \frac{T - T_3}{T - T_0} - \Lambda_+ \left(\frac{T - T_0'}{T_0'}\right)^{-p_+}\right]$$

$$= (q^2/\rho)\bar{c}_{11}^0 \frac{T - T_4}{T - T_0} \tag{15}$$

and

$$\Delta\omega_a^2 = (q^2/\rho)\Delta c_{11} , \tag{16}$$

respectively. Here, $\bar{c}_{11}^0$ and T_4 are parameters determined from a fit to the observed temperature dependence of c_{11}. In these equations, q is the absolute value of the phonon wave vector, ρ is the mass density of benzil, and γ is the damping constant for the acoustic phonon which shows a critical anomaly. Equation (14) has exactly the same form which has been traditionally used to exhibit the soft phonon/central peak response. [34,35] The susceptibility can be approximately decomposed into two contributions, one near the Brillouin peak at $\omega = \pm\omega_a$, the other near $\omega = 0$. To find the first contribution one assumes $\omega = \omega_a$. For the case $\omega\tau_e \gg 1$, one finds

$$\chi(q, \omega)_{Brillouin} \approx \frac{(q^2/\rho)}{\omega_a^2 + \Delta\omega_a^2 - \omega^2 + i\Gamma\omega} , \tag{17}$$

with an effective phonon width given by

$$\Gamma = \gamma + \Delta\omega_a^2/(\omega_a^2 \, \tau_e) \; .$$

Near $\omega = 0$, one finds

$$\chi(q, \omega)_{\text{Rayleigh}} \approx \frac{(q^2/\rho)(1 + i\omega\tau_e)}{\omega_a^2(1 + i\omega\tau_{\text{eff}})} \; , \tag{18}$$

with

$$\tau_{\text{eff}} = \tau_e(1 + \Delta\omega_a^2/\omega_a^2) \; . \tag{19}$$

The results for the susceptibilities near $\omega = \omega_a$ and $\omega = 0$, as given by Eqs. (17) and (18), are very similar to those which can be derived from a microscopic model of the effect of defects or impurities on the static and dynamic response, developed by Halperin and Varma.[25] Details are given in the Appendix. The present macroscopic description in terms of frequency dependent elastic constants seems, therefore, to be equivalent to the relaxing defect model of Halperin and Varma.

The light scattering structure factor in the high temperature limit[35]

$$S(q, \omega) = - (k_B T/\omega)\text{Im} \, \chi(q, \omega)$$

is then written as a sum of two parts:

$$S(q, \omega) = \frac{(k_B T q^2 \Delta\omega_a^2 \tau_e/\rho)}{\omega_a^4} (1 + \omega^2\tau_{\text{eff}}^2)^{-1}$$
$$+ \frac{(k_B T q^2 \Gamma/\rho)}{(\omega_a^2 + \Delta\omega_a^2 - \omega^2)^2 + \Gamma^2\omega^2} \; . \tag{20}$$

Here, the first part gives the central peak response and the second term the LA-phonon peak. In Eq. (20), the effective relaxation time is given by Eq. (19). Using Eqs. (15) and (16), as well as the fit of previous measurements of $c_{11} = c_{11}^R$ to Eq. (15),

$$c_{11} = (1.58 \times 10^{10} \, \text{N/m}^2)(T - 73.4)/(T - 72.6) \; ,$$

one finds

$$\tau_{\text{eff}} = \tau_e[1 + (\Delta c_{11}/c_{11}^0)(T - 72.6)/(T - 73.4)] \; . \tag{21}$$

In a similar manner, one can calculate the integrate intensity of the central peak as

$$I \propto \frac{(q^2/\rho) \, \Delta\omega_a^2}{\omega_a^4} = \frac{\Delta c_{11}}{(c_{11}^0)^2}\left(\frac{T - 72.6}{T - 73.4}\right)^2 \; . \tag{22}$$

The response of the annealed crystal also follows from Eq. (20) by taking the limit $\Delta\omega_a^2 \sim \Delta c_{11} \rightarrow 0$. It is seen that the central peak at $\omega = 0$, as given by Eq. (22), then disappears and only the Brillouin peak at $\omega = \omega_a$ and with width γ remains. This also follows from the Halperin–Varma theory as outlined in the Appendix, if the defect concentration c vanishes. Also, the temperature dependent anomaly for τ_{eff} disappears. For the unannealed crystal, Eq. (20) predicts slight changes in the Brillouin frequencies and linewidth from the original values of ω_a and γ to $\sqrt{\omega_a^2 + \Delta\omega_a^2}$ and $\Gamma = \gamma + \Delta\omega_a^2/(\omega_a^2 \, \tau_e)$, respectively. As discussed above, however, no such changes are observed; these differences probably fall within the experimental uncertainty.

Numerical calculations using the above expressions, assuming that Δc_{11} and τ_e are not functions of temperature, reproduce a weaker temperature dependence than the observed anomalies evidence. This is perhaps not surprising in view of the mean-field nature of our de-

scription.[25]

To test the theoretical relations given by Eqs. (19) and (22)

$$I \sim (\tau_{\text{eff}} - \tau_e)^2 = (\Delta\tau)^2 \tag{23}$$

with c_{11} constant around the transition temperature, we estimated the anomalous part of the effective relaxation time τ_{eff} by assuming τ_e possesses a monotonic temperature dependence through the phase transition as shown in Fig. 4 by the broken line. The calculated quantity $(\tau_{\text{eff}} - \tau_e)^2$ shows a sharp peak around the transition temperature and qualitatively reproduces the intensity anomalies observed in Brillouin and correlation scattering which are shown in Figs. 4 and 6.

The above result, that the intensity and square of the anomalous part of the relaxation time are proportional to one another, suggests that the observed central peak and correlation should be extrinsic effects generated by the motion of annealable defects in response to the external applied stress from the refrigerator. This clearly separates the present observations from the intrinsic anomalies found for KDP, KTS, and $Pb_5Ge_3O_{11}$. Without applied stress, no correlation function (relaxation process) could be observed: the defects will recover their intrinsic dynamics, relaxational or frozen, which the present light scattering experiments could not resolve, and the complex elastic constant becomes the real elastic constant. In this case, the theory predicts no central peak response and only the usual soft mode behavior is expected.

Of course, none of the above ideas or discussion precludes or denies in any way an intrinsic central peak behavior like that observed in KDP, KTS, etc., for benzil even if its origin is related to defect dynamics. In these reported experiments, however, no such intrinsic central peak dynamics could be observed.

The defect relaxation observed seems to occur only in response to the external applied stress from the refrigerator. One can introduce two defect states to describe the behavior of the defects following the applied stress: a relaxed or nonstressed state and a stressed or unrelaxed state. Transitions are caused between these two states by the external stress pulse only. Recall that the stress pulse can be thought of as a square wave with a rise time of tens of μs and an on time of roughly 100 ms. This conception of the present situation is completely analogous to the introduction of a spontaneous hopping of defects between two possible states in the crystal. In this sense, the externally induced central peak phenomenon can be seen as an example of the "relaxing defect cell" model in the theory of Halperin and Varma.[25] Once such a binary state system is introduced into the crystal, by whatever intrinsic (spontaneous) or extrinsic (external force induced) mechanism, a central peak response function follows for the system. This added defect degree of freedom is the essential feature of a defect induced central peak phenomenon. This is the major reason that the present theoretical results are parallel to the more usual[25] non-stress induced defect related central peak response function.

For the scattering geometry shown in Fig. 7 (sample II), the applied stress σ_3 in the ab plane induces a combination of strains,

$$\sigma_3 = c_{13}e_1 + c_{23}e_2 + c_{33}e_3 .$$

In this case, c_{11} has no low frequency dispersion or response. Moreover, the elastic constants appearing in the above expressions are not included in the elastic constants related to a-axis phonons.

Thus, the above developed theory gives a qualitative explanation of the observed defect related central peak and relaxation time found in this system. For a quantitative discussion of these phonomena, more precise measurements of the elastic anomalies, relaxation times, and Rayleigh intensity are required.

V. CONCLUSION

The a-axis polarized central peak observed in our previous Brillouin scattering experiments has been extensively studied by simultaneous measurement of Brillouin scattering and correlation spectroscopy. Our new findings are summarized as follows:

1. Correlation spectroscopy reveals a slow relaxation process in as grown samples only when an external stress is applied to the sample. On the other hand, well-annealed samples do not show the relaxation process under the same conditions.

2. The induced relaxation process can be observed in polarized scattered light and depends on the direction of the applied stress and on the observation direction.

3. The relaxation time and Rayleigh intensity show anomalies around the transition temperature, as revealed by the previous Brillouin experiments.

4. Brillouin shifts and elastic constants are found to be independent of the thermal treatment of samples to within the experimental uncertainty ($\sim 2\%$ for $\Delta\nu_B$, $\sim 4\%$ for c_{eff}).

These results suggest a possibility of annealable local stress fields due to defects or impurities in benzil generated during the processes of crystal growing and shaping. Some of these fields can be forced to deform and recover their shapes in response to an external applied stress pulse.

To formulate this idea more quantitatively, a complex elastic constant $c_{11}^*(\omega)$ is introduced through the theory of anelasticity. A dynamical susceptibility for LA phonons propagating along the [100] direction is discussed. This susceptibility can be approximately decomposed into a Rayleigh component which shows intensity divergence and critical slowing down of the relaxation time and a component which shows a pair of LA phonon responses. Within the theory, the central peak phenomenon can be related to an anomaly in the elastic constant c_{11}. The c_{11} anomaly arises from two separate contributions: a weak c_{66} anomaly and a strong anharmonic coupling between the strain $(e_1 + e_2)/2$ and fluctuations of the order parameters over wide temperature range ($T \lesssim T_c + 50$ K).

Although the theory qualitatively explains the ob-

served characteristic features, numerical calculations employing the previous results for the c_{11} anomaly reveal weaker divergences than are actually observed. The observed temperature dependence of the relaxation time is stronger than that estimated from the elastic anomaly. To improve the fitting, higher order interactions between the order parameters, including both the zone center and zone boundary modes, and various strains seem to be necessary.

The observed intensity anomaly in as grown crystals can be understood as an external applied stress induced effect. This phenomenon may also be modeled by the usual expression for the central peak response function which consists of a soft mode response with a relaxing self energy. Such an approach leads to the same expressions as those generated by the theory of anelasticity presented in this work. In this sense, there exists a strong relationship between the two approaches to central peak behavior. The central peak response function also predicts a relation $I \propto (\Delta\tau)^2$ between the intensity divergence and the relaxation time anomaly just as observed in these experiments.

Finally, a number of other samples have been studied and this phenomenon of a central peak in unannealed samples is not unique to benzil. Chloranil and urea show similar effects while NH_4Cl and triazine do not. Such observations are, of course, related to intrinsic (anisotropic) dynamics, defect concentration, and defect nature. These additional observations will be published in the near future.

After submission of this manuscript, a paper appeared dealing with x-ray diffuse scattering for benzil: H. Terauchi, T. Kojima, K. Sakaue, F. Tajiri, and H. Maeda, J. Chem. Phys. **76**, 612 (1982). These workers report critical diffuse scattering for both the zone boundary (M point) and zone center instabilities. These results support, in general, Toledano's predictions and our previous analysis of the c_{11} anomaly for benzil.

APPENDIX: COMPARISON WITH RELAXING DEFECT MODEL OF HALPERIN AND VARMA

The mean-field equations as developed by Halperin and Varma[25] which describe the response of a relaxing defect are, in their notation,

$$\sum_\beta [\delta_{\alpha\beta} - J_{\alpha\beta}(\mathbf{q}) \chi_\alpha(\omega)] y_\alpha(\mathbf{q}, \omega) = \chi_\alpha(\omega) h_\alpha(\mathbf{q}, \omega) . \quad (A1)$$

Here, $y_\alpha(\mathbf{q}, \omega)$ and $h_\alpha(\mathbf{q}, \omega)$ are the Fourier transforms of the particle displacement and the local external field, respectively. The indices α, β run over n and d to indicate normal and defect cells, respectively. For a concentration of defects c,

$$y_n = (1 - c)\psi_n$$

and   (A2)

$$y_d = c\psi_d .$$

In their model Halperin and Varma assume that the coupling constant between different n and d modes is independent of the indices n and d; that is, $J_{\alpha\beta}(\mathbf{q}) = J(\mathbf{q})$.

To apply the model of Halperin and Varma to the

present work, we instead assume

$$J_{nn}(\mathbf{q}) = J_{dd}(\mathbf{q}) = 0 ,$$

$$J_{nd}(\mathbf{q}) = J_{dn}(\mathbf{q}) = J(\mathbf{q}) . \qquad \text{(A3)}$$

Here, $J(\mathbf{q})$ represents the coupling between a particular (normal) phonon mode, with the susceptibility determined from

$$\chi_n^{-1} = \omega_a^2 - \omega^2 + i\gamma\omega \qquad \text{(A4)}$$

and a diffusive mode, to represent the defect motion, with a susceptibility given by

$$\chi_d^{-1} = k_B T(1 + i\omega\tau_e) . \qquad \text{(A5)}$$

Although it is apparent from the present work that the coupling $J(\mathbf{q})$ between the (normal) phonon modes and the defect motion depends strongly on phonon polarization and propagation direction, the details of this dependence remain to be elucidated. Releasing condition (A3) on the diagonal coupling terms would only result in a renormalization of the phonon susceptibilities and frequencies.

The various coupled susceptibilities are then calculated from Eq. (A1). For example, the phonon–phonon susceptibility, defined by

$$\chi_{nn} = \frac{\Psi_n}{h_n}\bigg|_{h_d = 0} \qquad \text{(A6)}$$

near $\omega = \omega_a$, is given by the same expression as Eq. (17) with

$$\Delta\omega_a^2 = \{c(1 - c)[J(\mathbf{q})]^2 q^2\}/(\rho k_B T) . \qquad \text{(A7)}$$

Near $\omega = 0$, one finds

$$\chi(\mathbf{q}, \omega)_{\text{Rayleigh}} \cong \frac{\dfrac{q^2}{\rho}(1 + i\omega\tau_e)}{(\omega_a^2 - \Delta\omega_a^2)(1 + i\omega\tau_{\text{eff}})} , \qquad \text{(A8)}$$

with $\Delta\omega_a^2$ given by Eq. (A7) and

$$\tau_{\text{eff}} \cong \left(1 + \frac{\Delta\omega_a^2}{\omega_a^2}\right)\tau_e . \qquad \text{(A9)}$$

This expression for the Rayleigh susceptibility becomes identical to Eq. (18) for $\Delta\omega_a^2 \ll \omega_a^2$.

The other contributions to the susceptibility of the coupled system, i.e., χ_{nd}, χ_{dn}, and χ_{dd}, have the same denominator as χ_{nn} and, therefore, can be expected to make qualitatively similar contributions.

[1]P. Esterich and B. E. Kohler, J. Chem. Phys. 59, 6681 (1973).

[2]Y. I. Chan and B. A. Heath, Chem. Phys. Lett. 46, 164 (1977).

[3]G. Odou, M. Mone, and V. Warin, Acta Crystallogr. Sect. A 34, 459 (1978).

[4]A. Dworkin and A. Fuchs, J. Chem. Phys. 67, 1789 (1977).

[5]J. Sapriel, A. Boudou, and A. Perigand, Phys. Rev. B 19, 1484 (1979).

[6]B. Wyncke, F. Buhat, and A. Hadni, Ferroelectrics 25, 617 (1980).

[7]R. Vacher, M. Boissier, and J. Sapriel, Phys. Rev. B 23, 215 (1981).

[8]A. Yoshihara, W. D. Wilber, E. R. Bernstein, and J. C. Raich, J. Chem. Phys. 76, 2064 (1982).

[9]J. C. Toledano, Phys. Rev. B 20, 1147 (1979).

[10]T. Riste, E. J. Samuelson, K. Otnes, and J. Feder, Solid State Commun. 9, 1455 (1971).

[11]For a recent review on these subjects, see A. D. Bruce and R. A. Cowley, Adv. Phys. 29, 219 (1980).

[12]N. C. Lagakos and H. Z. Cummins, Phys. Rev. B 10, 1963 (1974).

[13]M. D. Mermelstein and H. Z. Cummins, Phys. Rev. B 16, 2177 (1977).

[14]N. C. Lagakos and H. Z. Cummins, Phys. Rev. Lett. 34, 883 (1975).

[15]L. N. Durvasula and R. W. Gammon, Phys. Rev. Lett. 38, 1081 (1977).

[16](a) E. Courtens, Phys. Rev. Lett. 39, 561 (1977); (b) 41, 1171 (1978); (c) 47, 868 (1981).

[17]E. Courtens and R. W. Gammon, Phys. Rev. B 24, 3890 (1981).

[18]T. Yagi, H. Tanaka, and I. Tatsuzaki, Phys. Rev. Lett. 38, 609 (1977).

[19]H. Tanaka, T. Yagi, and I. Tatsuzaki, J. Phys. Soc. Jpn. 44, 1257 (1978).

[20]P. A. Fleury and K. B. Lyons, Solid State Commun. 32, 103 (1979); Phys. Rev. Lett. 37, 1088 (1976); K. B. Lyons and P. A. Fleury, Phys. Rev. B 17, 2403 (1978).

[21]G. J. Coombs and R. A. Cowley, J. Phys. C 6, 121 (1973); R. A. Cowley and G. J. Coombs, ibid., 6, 143 (1973).

[22]K. B. Lyon, R. C. Mockler, and W. J. O'Sullivan, J. Phys. C 6, L420, (1973); N. C. Lagakos, Ph. D. thesis (New York University, 1975).

[23]T. Shigenari, Y. Iimura, and Y. Takagi, Opt. Commun. 31, 57 (1979).

[24]D. J. Lockwood, J. W. Arthur, N. Taylor, and T. J. Hosea, Solid State Commun. 20, 703 (1976).

[25]B. I. Halperin and C. M. Varma, Phys. Rev. B 14, 4030 (1976).

[26]W. D. Ellenson and J. K. Kjems, J. Chem. Phys. 67, 3619 (1977).

[27]A. Yoshihara, C. L. Pan, E. R. Bernstein, and J. C. Raich, J. Chem. Phys. 76, 3218 (1982).

[28]G. D. Patterson and C. P. Lindsey, J. Chem. Phys. 70, 643 (1979).

[29]B. Chu, Laser Light Scattering (Academic, New York, 1974).

[30]J. C. Raich and E. R. Bernstein, J. Chem. Phys. 73, 1955 (1980).

[31]W. Rehwald, Adv. Phys. 22, 721 (1973).

[32]A. S. Nowick, in Physical Acoustics, edited by W. P. Mason and R. N. Thurston (Academic, New York, 1977), Vol. 13.

[33]R. Vacher and L. Boyer, Phys. Rev. B 6, 639 (1972).

[34]See, for example, J. Feder in Local Properties at Phase Transitions, edited by K. A. Muller and A. Rigamonti (North-Holland, Amsterdam, 1976), and Ref. 11.

[35]R. A. Cowley, Adv. Phys. 29, 1 (1980).